The Helical Structure of Sweat Ducts: Their Influence on the Electromagnetic Reflection Spectrum of the Skin

Itai Hayut, Alexander Puzenko, Paul Ben Ishai, Alexander Polsman, Aharon J. Agranat, and Yuri Feldman

***Abstract*—The helical structure of human eccrine sweat ducts, together with the dielectric properties of the human skin, suggested that their electromagnetic (EM) properties would resemble those of an array of helical antennas. In order to examine the implications of this assumption, numerical simulations in the frequency range of 100–450 GHz, were conducted. In addition, an initial set of measurements was made, and the reflection spectrum measured from the skin of human subjects was compared to the simulation results. The simulation model consisted of a three layer skin model (dermis, epidermis, and stratum corneum) with rough boundaries between the layers and helical sweat ducts embedded into the epidermis. The spectral response obtained by our simulations coincides with the analytical prediction of antenna theory and supports the hypothesis that the sweat ducts can be regarded as helical antennas. The results of the spectrum measurements from the human skin are in good agreement with the simulation results in the vicinity of the axial mode. The magnitude of this response depends on the conductivity of sweat in these frequencies, but the analysis of the phenomena and the frequencies related to the antenna-like modes are independent of this parameter. Furthermore, circular dichroism of the reflected electromagnetic field is a characteristic property of such helical antennas. In this work we show that: 1) circular dichroism is indeed a characteristic of the simulation model and 2) the helical structure of the sweat ducts has the strongest effect on the reflected signal at frequencies above 200 GHz, where the wavelength and the dimensions of the ducts are comparable. In particular, the strongest spectral response (as calculated by the simulations and measured experimentally) was noted around the predicted frequency (380 GHz) for the axial mode of the helical structure.**

***Index Terms*—Electromagnetic (EM) simulations, skin, sub-mm wave band, sweat ducts.**

I. Introduction

With the advent of modern imagery of living human skin, using methods such as optical coherence tomography (OCT), it was found that the human eccrine sweat duct has a well defined helical structure [1], [2]. This brought forward the hypothesis that the sweat ducts could exhibit electromagnetic (EM) behavior reminiscent of an array of helical antennas. This concept was presented and experimentally explored in two previous works, where changes in the electromagnetic reflection of the skin were observed as a result of elevated activity of the sweat glands, in a frequency range of 70–110 GHz [3], [4]. It is reasonable to assume that the morphology and electromagnetic properties of the skin have an impact on the reflected signal in this frequency range, as well as in higher frequencies in the sub-millimeter regime. To explore this assumption one must consider the structure of the skin.

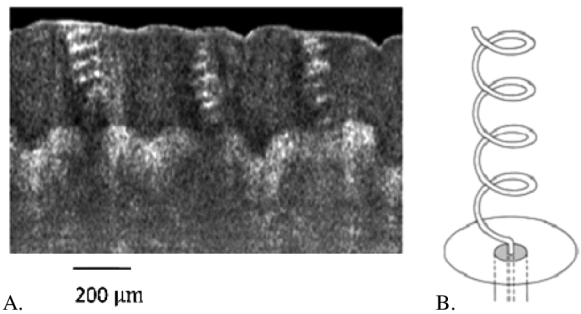

Fig. 1. Optical coherent tomography imaging of (a) the human skin (**reproduced with permission from ISIS GmbH**) and (b) a sketch of a helical antenna (see Balanis [12], **reproduced with permission from John Wiley & Sons Ltd.**). The helical sweat ducts are embedded within the epidermis. The roughness between the epidermis and the dermis is of the same order of magnitude as the sweat ducts length.

We consider a skin model, which is composed of different layers: 1) outermost stratum corneum (SC); 2) intermediate epidermis; and 3) inner dermis. For the purposes of investigating its electromagnetic response it is necessary to take into account the conductivity and permittivity values of each layer. This can be achieved by evaluating the bulk and bound water content in each layer (previously detailed in [4]).

One of the principal roles of the human skin is the thermoregulation of the body by sweat evaporation. Sweat is produced in the glands, located at the bottom of the dermis layer. The eccrine glands are the most common type of sweat glands, and are distributed through most of our body [5].

When activated by the nervous system the eccrine glands secrete the sweat liquid into the ducts—a tube-like micro organ. The ducts deliver the sweat up to the skin surface, where it evaporates through a pore in the SC [6].

The upmost section of the ducts associated with the eccrine glands have a well-defined helical structure [1], [2] as can be seen in Fig. 1. Histological studies have shown that about 90% of the sweat ducts are right-handed spirals [7].

In the sweat, the proton hopping can be considered as a mechanism for ultra-fast electrical charge mobility. Past studies have

Manuscript received July 12, 2012; revised August 28, 2012; accepted October 26, 2012. Date of publication December 28, 2012; date of current version February 27, 2013. This work was supported by the Israeli Ministry of Science under Grant 3/4602.

The authors are with the Department of Applied Physics, The Hebrew University of Jerusalem, 91904, Jerusalem, Israel (e-mail: yurif@vms.huji.ac.il).

Digital Object Identifier 10.1109/TTHZ.2012.2227476

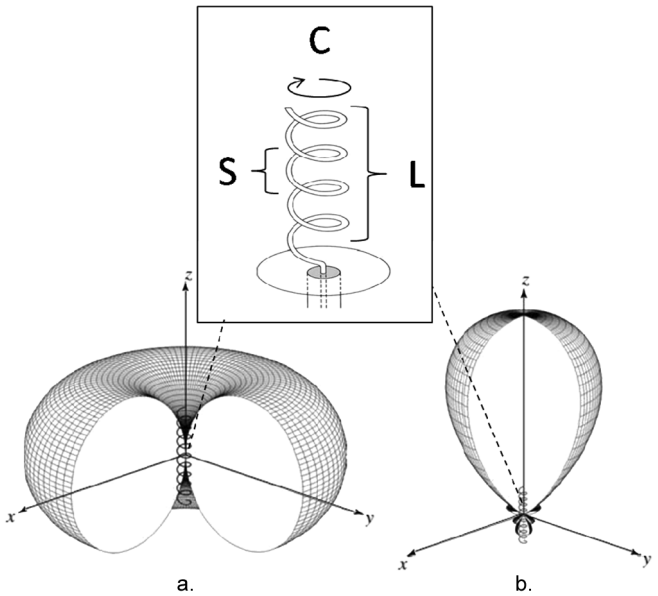

Fig. 2. Three-dimensional power patterns for (a) normal node and (b) axial (also called end-fire) mode. Based on (see Balanis [12], **reproduced with permission from John Wiley & Sons Ltd.**).

shown that the hopping timescale of protons in water is approximately 10–13 s [8], [9], allowing the creation of an alternating current in the sub-THz frequency band. In addition, using macroscopic measurements of electrolyte solutions [10] the conductivity of the sweat liquid, in the sub-THz frequency band, can be estimated to be at least 100 S/m in bulk solution. These findings confirm that the sweat ducts AC conductivity is much higher than the conductivity of the surrounding tissue in which the duct is embedded. Consequently, the helical structure of the sweat ducts and their electrical properties allow us to treat the EM response of the skin organ by adopting terminology and models taken from antenna theory. In these terms the sweat ducts can be regarded as an ensemble of helical antennas embedded in the skin dielectric medium.

A helical antenna is a device used for radiating or receiving EM waves, consisting of a conducting wire wound in the form of a helix. It was first presented by Kraus [11] and is broadly used in the communication industry. This antenna can be regarded as a hybrid between two elements: a dipole antenna and a loop antenna. Consequently, the helical antenna has two main modes of activation—a normal mode and an axial (end-fire) mode [12]. In the normal mode the helix acts much like a half-wave dipole antenna, effectively operating when the total length of the helix is smaller than the wavelength. In this mode the helix is radiating at an angle of 90° to the long axis of the helix [Fig. 2(a)]. However, unlike the dipole antenna the radiated field is elliptically polarized. In the axial mode, a resonance is created when the helix loop circumference equals the wavelength, and the spacing between loops is around quarter of the wavelength. The radiation is emitted from the antenna in the direction of the long axis [Fig. 2(b)]. In this mode the electromagnetic field radiated is circularly polarized, with the same chirality (left-hand or right hand polarization) as the helix.

In this work the relevant mode is the axial mode, because of the null electric field of the normal mode in the direction of the helix axis (perpendicular to the skin surface).

The geometrical conditions for the axial activation mode can be summarized by the relationships $C \approx \lambda$ and $S \approx \lambda/4$, Where C is the helix loop circumference, S is the spacing between loops and λ is the wavelength. In spite of the fact that the accurate geometrical dimensions of the helix contribute to the radiating efficiency, one can consider this mode valid even in the case of deviations from the exact values due to its broad bandwidth [12].

S-matrix formalism can be used to describe a general case where a local reference system is used to describe both incident and scattered waves. In particular, the propagation of a plane wave in an inhomogeneous media can be described in terms of a 4×4 scattering matrix, by which two orthogonal polarizations are taken into account [13]. In the special case of the same polarization of the incidence and the scattered waves, the problem can be reduced to a 2×2 scattering matrix, $S(\omega)$, where $\omega = 2\pi f$ and f is the frequency [13]:

$$S(\omega) = \begin{pmatrix} S_{11}(\omega) & S_{12}(\omega) \\ S_{21}(\omega) & S_{22}(\omega) \end{pmatrix}. \tag{1}$$

Here, the element $S_{11}(\omega)$ is the reflection coefficient equal to the ratio of the complex magnitudes of the reflected plane wave, $U_{ref}(\omega)$, to incident plane waves, $U_{in}(\omega)$:

$$S_{11}(\omega) = \frac{U_{\mathrm{ref}}(\omega)}{U_{in}(\omega)} \tag{2}$$

Similarly, the electromagnetic spectra of reflection and absorption from the human skin in the sub-mm wavelength band can be presented in terms of the matrix of scattering. The $S_{11}(\omega)$ term will describe the simulation results dealing with the reflection from a multi-layered skin model. Since the incident plane wave impinges normally on the skin, these results can be presented regardless of polarization.

In order to describe the frequency-dependant polarization changes, a different approach can be used. In general, the value of Circular Dichroism, $CD(\omega)$, is defined as the difference between left and right circular polarizations

$$CD(\omega) = \frac{\left(S_{11}^{\mathrm{LHCP}}(\omega) - S_{11}^{\mathrm{RHCP}}(\omega)\right)}{S_{11}(\omega)}. \tag{3}$$

It can be considered as a measure of the elliptical polarization of the reflected field. Here $S_{11}^{\mathrm{LHCP}}(\omega)$ is the left-handed circularly polarized reflection coefficient in a system excited by a linearly polarized source, and $S_{11}^{\mathrm{RHCP}}(\omega)$ is the right-handed circularly polarized reflection coefficient in a system excited by a linearly polarized source.

The initial set of simulations [3], [4] modeled the skin as a 3-layer planar system, where the boundaries between the layers were well-defined topologically flat planes. This was acceptable because the wavelength involved was larger than the dimension of roughness of boundaries between the layers ($\sim$0.5 mm). However, once higher frequencies are considered the roughness of the boundary must be incorporated into the model because both wavelength and roughness will be of the same order of magnitude.

The methodology adopted to evaluate EM wave propagation in the skin, consisted of applying finite elements (in frequency domain) or finite difference (in time domain) analysis to solve

the Maxwell equations throughout the three layers medium, in which the conducting helices were embedded (using CST microwave studio software).

In our previous studies the interface between the layers was considered to be flat [3]. This led to the creation of a standing wave between the layers, causing the absorption of the skin to be elevated near specific frequencies. The S_{11}-parameter magnitude at these frequencies was highly correlated with the expected sweat ducts activity (this elevated activity was due to physical stimulus), which was considered to be the main factor for creating changes in the electromagnetic properties of the epidermis. This frequency-dependent reflection of the skin at the frequency band 75–110 GHz was also experimentally observed [3].

Following our previous works [3], [4], other groups have exploited a similar skin model in order to examine the EM reflection [14]–[16] and energy absorption [17] of the skin in the sub-mm wavelength range.

Ney and Abdulhalim [14] suggested that spectral variations from the skin can be explained by interference between the skin layers, where the broad dielectric properties of the layers are changed. However, this idealized approach ignores the physiological behavior of human skin, by proposing a dramatic change in the dielectric permittivity of the epidermis. Furthermore, a recent study has confirmed that sweat ducts do play a key role in characterizing the spectral response of skin reflectivity [16]. The difficulty in determining and separating the influence of different structural properties on the reflected signal has motivated us to examine effects which can be created only by the unique helical structure.

In this work, we shall study the behavior of EM waves traversing through the skin. In addition to the studied simulation models [3], [4], [14]–[16] we will focus here on the 100–450 GHz frequency band, where the wavelength is equivalent to the dimensions of the helical structures. We shall consider a schematic model of the skin that takes into account the main details of its morphology and the dielectric response of its various layers including the rough boundaries between the skin layers, and the electrical properties of the sweat ducts. We explored for the first time a unique asymmetry created between left and right circular polarization of the reflected signal as a result of the natural dichroism of the human sweat ducts. We outline the frequency bands which are expected to guide experimentalists in the study of the electromagnetic response of the human skin. The suggested effect of sweat ducts on the spectrum can be used in order remotely sense an activation of the human sweat system, and can lead to the creation of a generic method for remote sensing of the physical and emotional state of human beings.

II. Models and Methods

A. The Model

As is clearly evident from the recent OCT images of the skin [1], [2], the interface between the layers is not flat. The dermal ridges penetrate into the epidermis as papillae, which can be almost as large as the thickness of the epidermis itself (Fig. 1). In this work, the non-flat boundary between the layers was taken into account, making the model more physiologically plausible. The boundary between the dermis and the epidermis was modeled as a two-dimensional sinusoidal surface (with amplitude of 350 μm). This was augmented by additional roughness at the upper boundary of the epidermis (between the epidermis and the SC) with amplitude of 50 μm. Adopting a non-flat interface between the layers was found to be effective for avoiding parasitic interference effects between the layers.

TABLE I
Skin Dielectric Parameters as Used in the simulations model. The AC Conductivity of the Sweat Ducts is Considered to be Much Higher Than That of its Surrounding Epidermis

Component	Relative Permittivity	AC Conductivity (S/m)
Dermis	3.9	30
Epidermis	3.2	1
Stratum cornea (SC)	2.4	10^{-5}
Sweat duct	4	100-10000

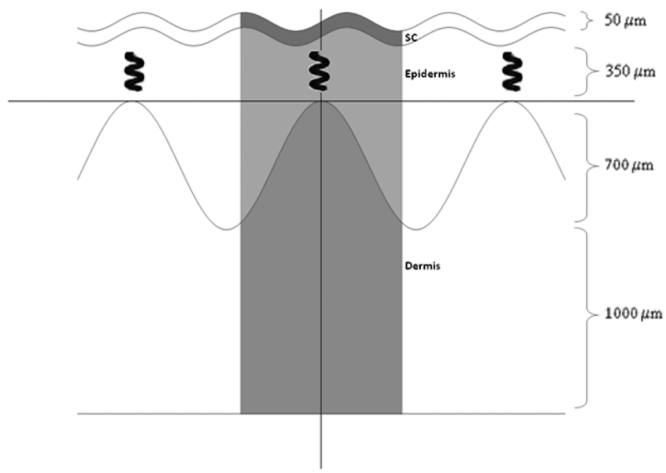

Fig. 3. The model side cross-section. The skin is divided into three layers: stratum corneum (SC), epidermis and dermis. The helical sweat ducts are located in the epidermis. Sinusoidal functions with different spatial frequencies and amplitudes are used in order to model the non-flat boundaries between the dermis, epidermis and SC.

The periodical shape of the layer boundaries, although supported by the morphology of the human skin (Fig. 1), does not play an important role in shaping the electromagnetic spectral response. The different components of the skin were modeled using the same dielectric properties as calculated in previous studies [4]. The conductivity of the sweat ducts was considered to be much higher than that of the skin layers, varying between zero in the absence of sweat ducts activity to 100–10 000 S/m [3], [4], [10], which might account for the different activation states of the sweat system in response to neurophysiologic stimuli. The model parameters are summarized in Table I and Fig. 3.

B. Computation Method

The EM simulation was conducted using the CST Microwave Studio software package, utilizing a 3-D finite-difference or finite-element analysis to solve Maxwell's equations over a mesh

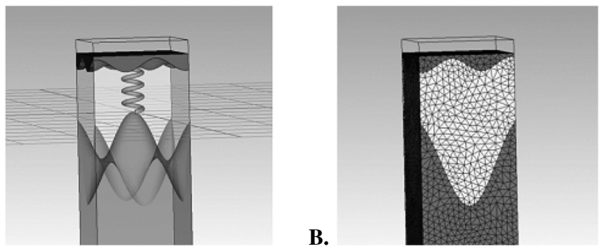

Fig. 4. The 3-layer skin model. The simulation is conducted over the (a) unit cell using (b) tetrahedral mesh. Periodic boundary conditions extend the model into the surrounding space.

of cells covering the model. A typical method for carrying out such simulations is the use of a waveguide port generating an electromagnetic pulse which propagates in the simulated space. The reflection from the simulated system is computed and the spectrum is calculated using fast Fourier transform (time-domain calculation).

In this work a different method was applied—the model was simulated using finite-element analysis as a frequency-selective surface (FSS). A FSS may be viewed as a filter of electromagnetic waves in the frequency domain [18]. A single model element is built within a unit cell. The unit cell boundary conditions virtually repeat the modeled structure periodically in the two directions along the skin surface up to infinity. An excitation source of the normal incidence plain waves was placed on the axis perpendicular to these two directions. At this port the differences between the outgoing and incoming electromagnetic radiation was measured in order to calculate the S-parameters. The unit cell was defined as containing one sweat duct. The same structure was replicated in the neighboring cells through the periodic boundary conditions (Fig. 4). Such a periodic structure allows the use of Floquet's theorem in the computation process [19]. This results in a reduction of the simulation domain, causing a significant shortening of the computation time. The concentration of ducts in the skin was modified by changing the size of the unit cells, effectively changing the distance between the ducts (see Section III). The FSS method allowed us to decrease the model size calculated, and therefore to use a highly accurate mesh (about 100 000 tetrahedrons in one unit cell, each duct is built of 100–500 tetrahedrons).

The use of tetrahedral mesh was found to be computationally efficient due to the curved nature of the helical sweat ducts. The periodic boundary conditions were found to be effective in avoiding reflections from the model edges. In addition, using the plane wave source eliminated parasitic effects due to the creation of a standing wave between the port and the model.

In order to calculate the results for circular dichroism in the reflected signal, a slightly different model was used, due to software limitations: The model was built as a complete skin fragment containing five sweat ducts (Fig. 5), and the computation was made using a pulse excitation source (via a time-domain calculation). The electromagnetic reflected field at a large distance perpendicular to the skin surface (far field) was calculated, and the left and right circular polarized components were compared.

Fig. 5. The skin model used in the circular dichroism simulation. This simulation was made using a pulse excitation source (time domain calculation).

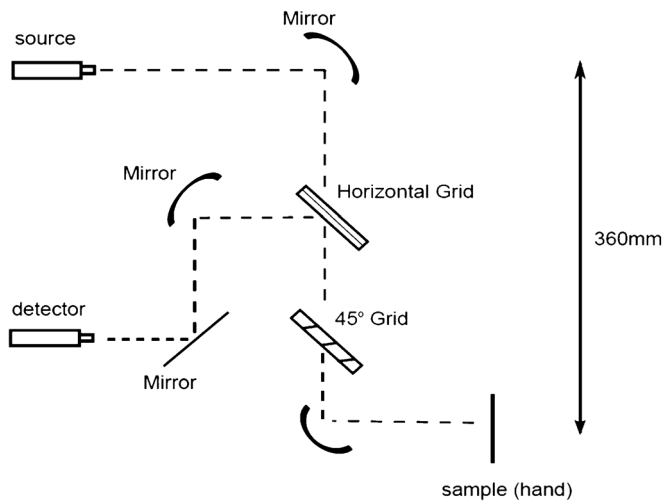

Fig. 6. Schematic representation of the AB-mm VNA measuring system. Arrows represent the propagation of the beam from the source to the sample and its reflection to the detector. A directional coupler is created by two polarizing grids, standing at 45 deg to each other.

C. Experimental Setup and Method

The reflection coefficient of the human palm was measured using an AB-Millimetre vector network analyzer (MVNA-8-350, Paris, France), described in [20]–[22], that can cover the frequency range from 8 to 660 GHz. The optical path in this setup from the source to the hand was 72 cm and the beam was focused with elliptical mirrors (see Fig. 6). The hand of the subject was fixed at the point of focus using a special holder designed to be of minimal inconvenience to the subject.

The right hand was placed into the holder with the bottom end of the palm situated at the beam focus. The reflection coefficient of the palm was then measured as the subject was at rest. The measurement was made in the ASA frequency band (260–440 GHz). The measured spectrum was divided into eight separate bands; in each one the appropriate configuration of the system was used. The recorded signal is computed in respect to a reference (a metal plate). Two subjects were measured, each one with repeating 11 frequency sweeps in every frequency band. The entire spectrum was then combined from the separate bands, in a

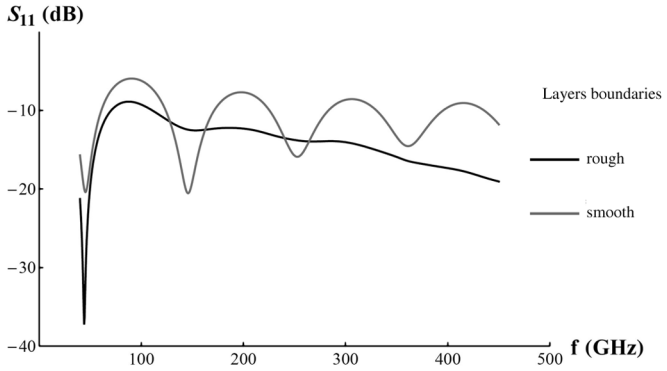

Fig. 7. The reflection spectra of two different models of the skin (without sweat ducts) were compared: A model with flat boundaries between the layers (grey) and a model including rough boundaries between the layers (black). The rough boundaries reduce the effect of standing waves on the reflection spectrum above 100 GHz.

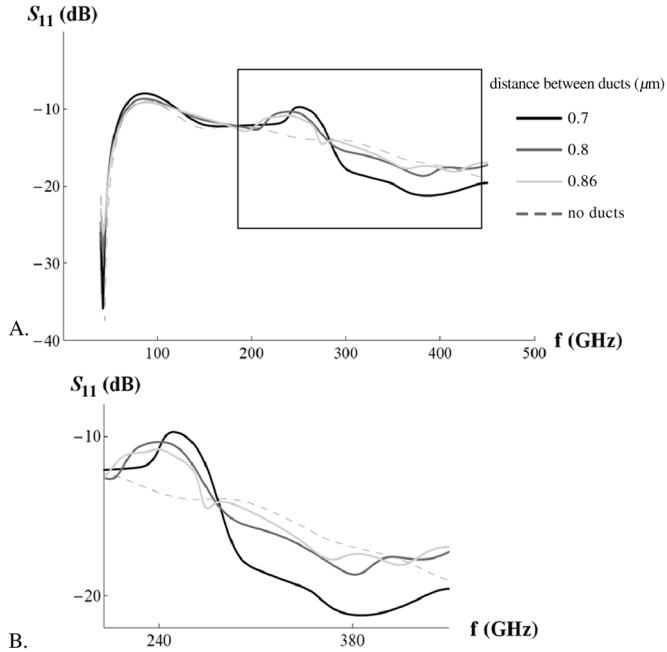

Fig. 8. Reflection spectrum from the skin model, for different values of distances between ducts. (A) Inter-layer interferometry minimum is created at the lower frequencies band (∼50 GHz). (B) The lower figure is a magnification of the spectrum in the frequency range of 200–450 GHz. The main resonance can be seen, corresponding to the axial mode (∼380 GHz). The conductivity value of the sweat ducts is fixed on the high-limit value of 10 000 S/m.

way that the last part of the first band was matched with the first part of the following band, etc. The data was then smoothed using a robust first-order polynomial local regression method (spanned locally on 5% of the data).

III. Results and Discussion

A. Effect of the Rough Layer Boundaries

Initially the skin model was simulated without ducts. The influence of the periodic rough layer boundaries on the reflection coefficient S_{11} was investigated. The results, presented in Fig. 7, show that at frequencies above 100 GHz the rough layer boundaries have reduced the interference in comparison with the flat boundaries, while the first interferential minimum (below 100 GHz) becomes more pronounced. The simulation results obtained in the low frequency range for the smooth boundaries without ducts coincide with similar results presented in the previous studies [3], [4], [14], [15] where flat boundaries between the layers were considered. The maximal epidermis thickness is increased due to the introduction of rough boundaries, so that the maximal thickness is 1050 μm instead of 350 μm for the flat boundaries model. This yields a creation of the first minima at 50 GHz compared to 90 GHz in the previous studies.

B. Helical Sweat Ducts Response Modes

The frequency of the axial mode of the helical ducts embedded in the skin model have been estimated by means of antenna theory, using $\varepsilon \cong 3.2$ for the relative permittivity of the epidermis layer, in which the ducts are embedded.

As the wavelength approaches the size of the circumference of the duct, we expect the emergence of the axial-mode resonance, the frequency of which is given by:

$$C \approx \lambda \Rightarrow f_{\text{axial}} \approx \frac{\frac{c_0}{\sqrt{\varepsilon}}}{C} \approx 380 \text{ GHz} \tag{4}$$

here c_0 is the speed of light in vacuum, and C is the duct circumference (we assume here $C \approx 140\pi$ μm). The loop spacing based on OCT images ($S = 87.5$ μm) slightly deviates from its optimal value ($S = 110$ μm) but as it was mentioned above, the axial mode activation in a helical antenna can still be considered [12]. In order to study the effect of the axial helix mode on the reflected field, a numerical simulation of the skin model with ducts was conducted (see computational method) and the $S_{11}(\omega)$ parameter was calculated. At this stage the ducts surface density, which depends on the distance between the ducts, was the only parameter of the model that was varied. Results of the calculations of the spectra of the reflection coefficient modulus $|S_{11}|$, for different distances between the ducts are plotted in Fig. 8. The notable spectral variations when the distances between ducts are changed can be observed in the vicinity of the estimated resonance frequency for the axial mode. Since the values of the sweat duct length and its circumference are comparable, there might be also an influence of the total duct length. This can relate to a normal mode, although such effect should be very small in the direction perpendicular to the skin surface. Antenna theory analysis implies that the axial mode dominates at a frequency of ∼380 GHz.

The results also show that the distance between the ducts has limited effect on the location (in frequency domain) of the regions of spectral variations. This leads to the conclusion that the frequency-dependent response is not related to ducts coupling. This is probably due to a strong attenuation of the EM field in the epidermis at these frequencies, which decreases the EM amplitude in the normal direction of the ducts. Besides the distance between the ducts and the thickness of the epidermis, the only length sizes of the model, which corresponds to the wavelength range of 100–450 GHz, are related to the helical structure itself.

The fact that the reflectance is elevated at ∼240 GHz and reduced at ∼380 GHz is due to phase differences in the reflected

electromagnetic field. When charges flow between the upper and the lower parts of the duct, a rotating current is also created in the circumference of the duct as well. This induces an electromagnetic wave propagating on the direction perpendicular to the skin surface. The field radiated from the ducts is combined with the field that is reflected from the skin surface, and the phase between these two waves will determine whether the reflection will be elevated or decreased.

C. Dependence of the Spectral Response on the Conductivity

The sweat ducts conductivity was chosen as the parameter by which the sweat glands and ducts activity is modeled. It is well known that arousal of the human central nervous system encourages the excretion of sweat from the sweat glands and transporting it to the skin surface through the sweat ducts [23]–[25]. This leads to alteration of the quantity and composition of the sweat in the ducts, which contributes to their AC conductivity. Hence, changes in the conductivity of the ducts can be used as a reasonable model for investigating the effect of the sweat system activation on the reflection spectrum. One must ask what are, in this case, the limits of the AC conductivity? In bulk water σ_{AC} can be estimated using the dielectric losses, $\sigma'(\omega) = \omega(\varepsilon_0\varepsilon''(\omega) + \sigma_{\mathrm{DC}}/\omega)$, where the DC element is assigned to mostly proton hopping [26]. As this is a diffusive motion it can be estimated by $\sigma_{\mathrm{DC}} = \mathrm{Ne}^{+}\mu_{\mathrm{H}^+}$, where N is the proton concentration, e^+ the elementary proton charge and μ_{H^+} is the proton mobility (linked to the diffusion coefficient, D_{H^+} by the Einstein relationship $\mu_{\mathrm{H}^+} = D_{H^+}/kT$, [27]). At 100 GHz this estimation gives approximately 100 S/m at [28]. Note, that the similar value of conductivity was measured in the solution of simple electrolyte KCl and NaCl at a frequency of 40 GHz, in the concentration range of 0.01 to 1 mol/l at a room temperature [10], and would be even higher at 100 GHz. However, the diffusion coefficient of protons has been demonstrated to increase once water becomes ordered. For instance the diffusion coefficient of protons in ice is 10 times higher than of protons in bulk water at room temperature [29]. Furthermore there is evidence to suggest that in the vicinity of a lipid/water interface, water is highly structured [30] and that along such structures fluorescence spectroscopy estimated an increase in proton diffusion by a factor of 100 [31] in comparison to that of protons in the bulk water. The layer of "ordered" water in the duct is approximately a few nanometers deep [32], is small compared to the micrometers diameter of the duct itself. Consequently the ratio of volumes is of the order of 0.01. Under the assumption of a radial homogeneity in proton density inside the sweat duct, the contribution from proton hopping along the duct surface can be estimated by a similar weighting and therefore not negligible. Using the value of dielectric losses for water ($\varepsilon'' = 6$) and for ice (almost zero) at 300 GHz [33], the ratio of conductivities between the surface layer and the bulk is given by

$$\frac{\sigma_l'(\omega)}{\sigma_b'(\omega)} = \frac{(\varepsilon_0\varepsilon_l''(\omega) + \sigma_l/\omega)}{(\varepsilon_0\varepsilon_b''(\omega) + \sigma_b/\omega)}$$

which can be estimated by

$$\frac{\sigma_l'(\omega)}{\sigma_b'(\omega)} = \frac{(100Ne^{+}\mu_{H^+})}{(6\varepsilon_0\omega + \mathrm{Ne}^{+}\mu_{\mathrm{H}^+})}.$$

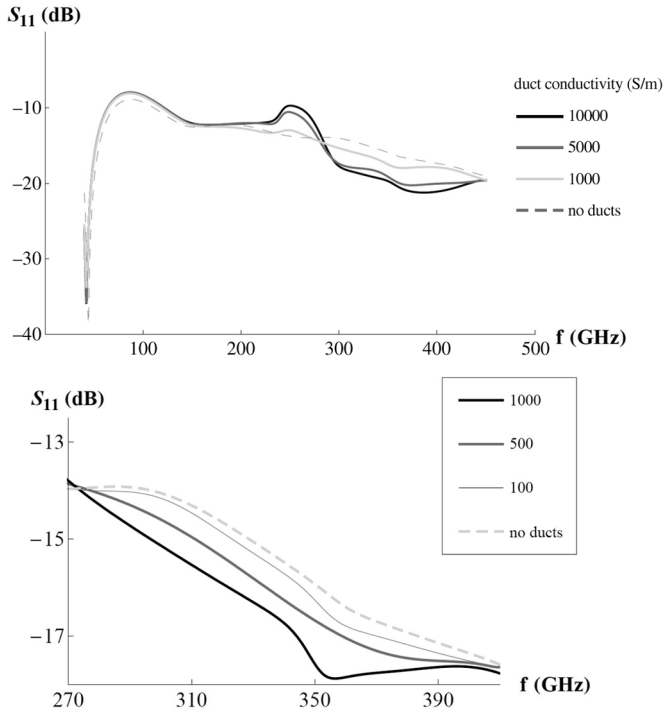

Fig. 9. (top) The reflection spectrum from the skin model for different values of the conductivity of the helical sweat ducts, with constant distance between ducts of 700 μm. The frequency regions in which helical sweat ducts affect the spectrum does not change when the conductivity is modified. (bottom) For moderate conductivity values, the effect of the sweat ducts is less pronounced, but peak differences still corresponds to the axial mode (∼380 GHz).

Using the values of [34] for the proton conductivity in bulk water as a function of the proton concentration we have for a concentration of 1 mole [H+] [H+] $Ne^{+}\mu_{\mathrm{H}^+} \sim 1$ S/m. Consequently the ratio of the respective surface and bulk conductivities is $\sigma_l'(\omega)/\sigma_b'(\omega) \sim 100$. Given that bulk water conductivity is 100 S/m and that for an electrolyte solution it is even higher, it is not unreasonable to set the upper limit of conductivity as 10,000 S/m. Hence, most of the simulations were made using the upper limit of the theoretical conductivity values of sweat (1000–10 000 S/m). However, the results are valid even with lower conductivities, as can be seen in Fig. 9 (lower). In fact, the main results of this paper (in terms of the spectral shape and antenna modes) are independent of the value of the sweat conductivity—as long as it is higher than that of the surrounding tissue. In short it is merely a signal-to-noise issue. Such an approach can also be used in order to predict the experimental results of electromagnetic reflection from human subjects with different levels of the thermoregulation system activity, as done previously [3].

In this work, the simulations with different conductivity levels have enabled us to identify the effect of the helical sweat ducts in the passive regime, i.e., without any possible additional modulation of the current by another source.

When the conductivity is increased, a prominent change in the reflectance spectrum was observed, especially in the vicinity of the axial mode resonance (350–400 GHz), which was discussed earlier in the paper (Fig. 9 (top)). This response region does not shift with changes in the conductivity. This fact supports the

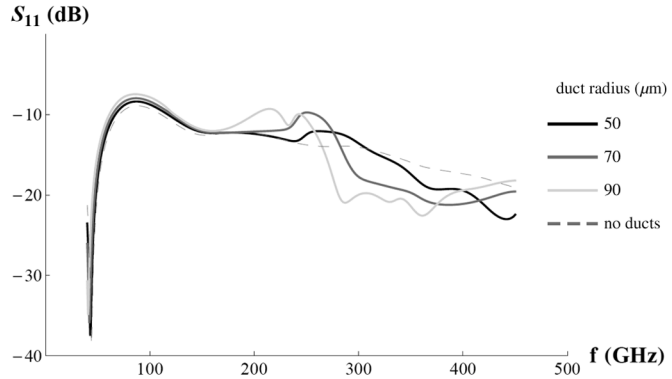

Fig. 10. The reflection spectrum from the skin model, for different values of the diameter of the helical sweat ducts. The axial mode frequency shifts as we change the duct diameter, as expected. . . The conductivity value of the sweat ducts is fixed on the high-limit value of 10,000 S/m.

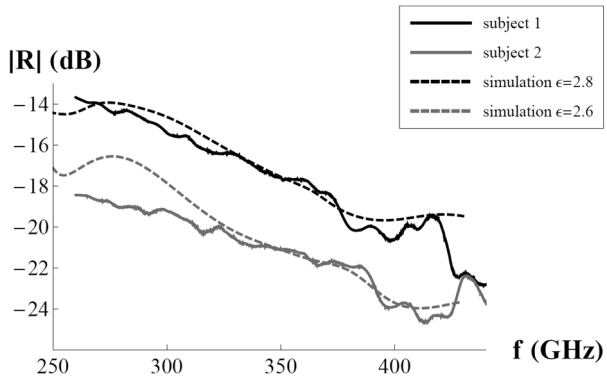

Fig. 11. The modulus of the reflection coefficient $|R|$ as measured from the skin of two subjects using the AB-mm VNA (solid lines) and as produced by the simulation model with different values of epidermis permittivity (dashed lines). In both measurement sets a significant change in the reflection spectrum was measured in the vicinity of the frequency region suggested as the axial mode ($\sim$380 GHz). The spectral shape is slightly different between the two subjects, as expected due to morphology variations between the skin of the subjects. The simulations were made using the parameters listed at Table I, except duct conductivity (1500 S/m in both simulations) and epidermis relative permittivity (2.6 and 2.8).

conclusion that this is the region of the spectral variations which emerges from the structural properties of the helical sweat ducts.

D. Spectral Response Dependence on the Ducts Circumference

According to antenna theory, a helical antenna axial mode center wavelength is equal to the circumference of the helix [11]. Therefore, changes in the circumference of the ducts in the simulation model should be followed by matching changes in the absorption peak location. As expected, the response band originally computed at 350–400 GHz shifts to higher frequencies when we decrease the diameter of the ducts and to lower frequencies when we increase it (Fig. 10). The reflection peak at 250–300 GHz also shifts when we change the diameter of the ducts, which is consistent with the assumption that this peak does not simply relates to a normal mode resonance of the ducts.

An explanation of this effect can be found in the fact that the "classic" antenna theory normal mode of a helix relates to a long and narrow helix [11], and this is not the case in our model. As mentioned above, the fact that the circumference and the height of the ducts are of the same order of magnitude creates this "impure" mode that relates to both height and diameter.

E. Experimental Measurement Results

The experimental results (See Fig. 11) give the first indication of a measurable enhanced spectral absorption in the region related to the axial mode ($\sim$380 GHz). Nevertheless, the elevated reflectance region from the simulation routine was not observed in the frequency band ($\sim$240 GHz) correspondent to the normal-mode. This might be due to the fact that the measurement was conducted only above 260 GHz, or that the spectral variation in this region is much weaker (than predicted in the simulations). The exact location of the absorption local maximum was slightly different between the two subjects, but the spectral shape was robust (in the limitations of an *in vivo* measurement) for each one of them separately. The shift in the reflection minimum can be achieved in the simulation spectrum or by changing the dielectric permittivity of the epidermis or varying the radius of the helical duct. Here a comparison of two simulations was made using different values of the epidermis dielectric permittivity (values of 2.6 and 2.8) and duct conductivity value of 1500 S/m, while all the other parameters remain constant according to Table I. Shift in the reflection minimum can also be acquired by changing the radius of the helical duct.

These measurements mark the starting point for future research, as a larger number of subjects and measurements can supply statistically-significant results in order to verify experimentally the simulations results. For such additional measurements, a time-domain system might be more appropriate, in order to avoid the separation of the frequency range into smaller bands as the VNA requires.

F. Circular Polarization

In principal, the helical structure of the sweat ducts implies that an electromagnetic radiation reflected from the skin must have specific polarization properties. Similar to the classical helical antenna, a helical sweat duct should have a strong response to a preferred circular polarization direction [11], [12]. At the macroscopic level, if the ducts turn direction was equally distributed to both directions, the sum of the reflected signal was averaged out and this property of the ducts would not be expressed. Remarkably, studies of the morphology of the human skin have clearly shown that about 90% of the sweat ducts are right-handed spirals [7]. When exciting the skin using linear electromagnetic radiation (which can be expressed as superposition of two equal left and right circular components), this asymmetry should be expressed in the reflected signal. In order to examine this phenomenon we used a similar skin model simulation and examined the difference between the left and right circular polarization components of the reflected field. The model was excited using a linearly polarized wave source, and the maximum amplitude of the reflected electric field was examined separately for left and right circular components. Plotting the difference between these two components, one can clearly see the circular dichroism in the same frequency bands related to the helix modes (Fig. 12). At frequencies lower than 200 GHz, the wavelength is larger than the dimensions of the ducts, and there is no difference between the two components. At these

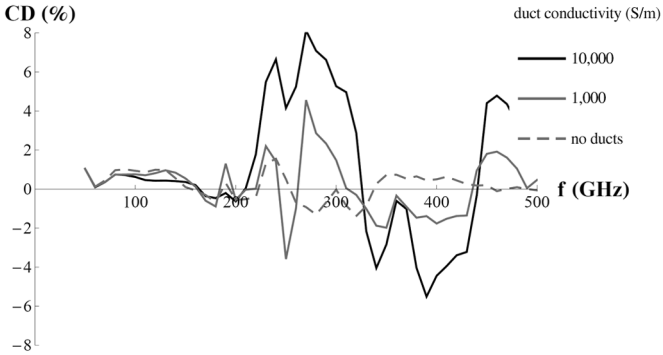

Fig. 12. CD (circular dichroism)—The difference between the left and right circularly polarized electromagnetic field amplitude in the reflected signal, as a percent from the total reflected electromagnetic field amplitude. CD appears when the wavelength approaches the structural dimensions of the sweat duct (>200 GHz).

long wavelengths, the fine helical structure of the ducts cannot be expressed, and so the difference between left and right components is zero. As the excitation wavelength approaches the size of the duct (around 200 GHz), the ratio between the left and right components starts to change. Circular dichroism reaches a high level around 350–400 GHz, as the ducts interact with the radiation close to their axial mode. Such a preference for a particular polarization direction might be detected experimentally, as sub-mm sources and detectors become more available.

IV. Conclusions

In this work, the details of the structure of the both the morphological features and the electrical conductivity of the sweat ducts were shown to have an important role in shaping the reflectance spectra of the human skin in the frequency band of 100–450 GHz. Unlike other skin modeling studies, it was shown here that the effect of multilayer interference is substantially reduced when the non-flat boundaries between the different skin layers are taken into account.

The performed simulations demonstrate that variations of the spectra are observed in the vicinity of the frequencies close to the predicted axial response mode of the sweat ducts (regarded as helical antennas) at approximately 380 GHz. In addition a lower frequency peak which appears around 240 GHz might be a result of an impure normal mode related to the total length of the helix. The results clearly show that the structure of the sweat ducts plays a key role in the shaping of the reflected spectra. It should be emphasized that the simulated passive model sweat ducts are excited only by the incident plane wave without any modulation of the current by additional sources. The simulation demonstrates that the frequency region of the main spectral variations does not depend on the conductivity value, as the increasing of conductivity only amplifies the effect.

In addition, due to the natural preference of the direction in the human sweat ducts chirality, the expected circular polarization effect was supported by the simulation. This effect is pronounced in the vicinity of the main spectral variations. In an initial set of measurements, the spectral variation in the vicinity of the axial mode was observed, supporting the hypothesis that the helical structure of sweat ducts influences the reflection spectrum of the human skin at sub-mm wavelengths. It is clear that this model have to be extended in the future for consideration of strong coupling between the sweat ducts, to take into account the stochastic nature of ducts morphology, and other parameters of our simplified model.

Acknowledgment

The authors thank Prof. V. Ilyin, Prof. V. Rozenshtein, L. Lavy, I. Segev, E. Safrai, and E. Na'aman for helpful discussions.

References

[1] A. Knuttel and M. Boehlau-Godau, "Spatially confined and temporally resolved refractive index and scattering evaluation in human skin performed with optical coherence tomography," *J Biomed Opt.*, vol. 5, pp. 83–92, Jan. 2000.

[2] A. Knuttel, S. Bonev, and W. Knaak, "New method for evaluation of IN VIVO scattering and refractive index properties obtained with optical coherence tomography," *J Biomed. Opt.*, vol. 9, pp. 265–273, Mar.–Apr. 2004.

[3] Y. Feldman, A. Puzenko, P. Ben Ishai, A. Caduff, and A. J. Agranat, "Human skin as arrays of helical antennas in the millimeter and submillimeter wave range," *Phys. Rev. Lett.*, vol. 100, p. 128102, 2008.

[4] Y. Feldman, A. Puzenko, P. Ben Ishai, A. Caduff, I. Davidovich, F. Sakran, and A. J. Agranat, "The electromagnetic response of human skin in the millimetre and submillimetre wave range," *Phys. Med. Biol.*, vol. 54, pp. 3341–3363, Jun. 7, 2009.

[5] H. R. Jacubovic and A. B. Ackerman, *Dermatology*, vol. 1, p. 66, 1992.

[6] L. A. Goldsmith, *Fitzpatrick's Dermatology in Internal Medicine*, vol. 1, p. 155.

[7] S. Takagi and M. Tagawa, "Predominance of right-handed spirals in the intraepidermial sweat ducts in man and the primates," *Japan. J. Physiol.*, vol. 7, p. 113, 1957.

[8] V. V. Krasnoholovets, P. M. Tomchuk, and S. P. Lukyanets, "Proton transfer and coherent phenomena in molecular structures with hydrogen bonds," in *Advances in Chemical Physics*. Hoboken, NJ: Wiley, 2003, pp. 351–548.

[9] M. A. Lill and V. Helms, "Molecular dynamics simulation of proton transport with quantum mechanically derived proton hopping rates (Q-HOP MD)," *J. Chem. Phys.*, vol. 115, pp. 7993–8005, 2001.

[10] R. Gulich, M. Kohler, P. Lunkenheimer, and A. Loidl, "Dielectric spectroscopy on aqueous electrolytic solutions," *Rad. Environ. Biophys.*, vol. 48, pp. 107–114, Feb. 2009.

[11] J. D. Kraus, *Antennas*. New York: McGraw-Hill, 1950, p. 382.

[12] C. A. Balanis, *Antenna Theory: Analysis and Design*, 3rd ed. Hoboken, NJ: Wiley, 2005.

[13] D. M. Pozar, *Microwave Engineering*. Hoboken, NJ: Wiley, 1998, p. 196.

[14] M. Ney and I. Abdulhalim, "Does human skin truly behave as an array of helical antennae in the millimeter and terahertz wave ranges?," *Opt. Lett.*, vol. 35, pp. 3180–3182, 2010.

[15] M. Ney and I. Abdulhalim, "Modeling of reflectometric and ellipsometric spectra from the skin in the terahertz and submillimeter waves region," *J Biomed. Opt.*, vol. 16, pp. 067006–15, 2011.

[16] B. Yang, R. S. Donnan, M. Zhou, and A. A. Kingravi, "Reassessment of the electromagnetic reflection response of human skin at W-band," *Opt. Lett.*, vol. 36, pp. 4203–4205, 2011.

[17] G. Shafirstein and E. G. Moros, "Modelling millimetre wave propagation and absorption in a high resolution skin model: The effect of sweat glands," *Phys. Med. Biol.*, vol. 56, p. 1329, 2011.

[18] D. CST Computer Simulation Technology AG, Darmstadt , Germany, "CST Microwave Studio suite—Ver. 2010," [Online]. Available: http://www.cst.com/Content/Applications/Article/A+Polarisation+Independent+Bandpass+FSS, Accessed Apr. 10, 2011

[19] W. Magnus and S. Winkler, "Floquet's theorem," in *Hill's Equation*. New York: Dover, 1979, vol. 1.2, pp. 3–8.

[20] A. Elhawil, G. Koers, L. Zhang, J. Stiens, and R. Vounckx, "Reliable method for material characterisation using quasi-optical free-space measurement," *IET Sci., Meas., Technol.*, vol. 3, pp. 39–50, 2009.

[21] M. Mola, S. Hill, P. Goy, and M. Gross, "Instrumentation for millimeter-wave magnetoelectrodynamic investigations of low-dimensional conductors and superconductors," *Rev. Sci. Instrum.*, vol. 71, pp. 186–200, 2000.

[22] S. Takahashi and S. Hill, "Rotating cavity for high-field angle-dependent microwave spectroscopy of low-dimensional conductors and magnets," *Rev. Sci. Instrum.*, vol. 76, p. 023114-10, 2005.
[23] D. M. DiPasquale, M. J. Buono, and F. W. Kolkhorst, "Effect of skin temperature on the cholinergic sensitivity of the human eccrine sweat gland," *Jpn. J. Physiol.*, vol. 53, pp. 427–430, Dec. 2003.
[24] S. C. Landis and D. Keefe, "Evidence for neurotransmitter plasticity in vivo: Developmental changes in properties of cholinergic sympathetic neurons," *Devices Biol.*, vol. 98, pp. 349–372, Aug. 1983.
[25] A. K. M. Shamsuddin and T. Togawa, "Continuous monitoring of sweating by electrical conductivity measurement," *Physiol. Meas.*, vol. 19, p. 375, 1998.
[26] D. S. Eisenberg and W. Kauzmann, *The Structure and Properties of Water*. Oxford, U.K.: Clarendon, 1969.
[27] R. K. Pathria, *Statistical Mechanics*, 1st ed. New York: Pergamon, 1972.
[28] S. Cukierman, "Proton mobilities in water and in different stereoisomers of covalently linked gramicidin A channels," *Biophys. J*, vol. 78, pp. 1825–1834, Apr. 2000.
[29] I. Presiado, J. Lal, E. Mamontov, A. I. Kolesnikov, and D. Huppert, "Fast proton hopping detection in ice Ih by quasi-elastic neutron scattering," *J. Phys. Chem. C*, vol. 115, pp. 10245–10251, May 2011, 2011.
[30] J. Kim, W. Lu, W. Qiu, L. Wang, M. Caffrey, and D. Zhong, "Ultrafast hydration dynamics in the lipidic cubic phase:? Discrete Water Structures in Nanochannels," *J. Phys. Chem. C*, vol. 110, pp. 21994–22000, Nov. 2006, 2006.
[31] M. Brändén, T. Sandén, P. Brzezinski, and J. Widengren, "Localized proton microcircuits at the biological membrane-water interface," *Proc. Nat. Acad. Sci.*, vol. 103, pp. 19766–19770, Dec. 2006, 2006.
[32] M. Simeonova and J. Gimsa, "The influence of the molecular structure of lipid membranes on the electric field distribution and energy absorption," *Bioelectromagn.*, vol. 27, pp. 652–666, 2006.
[33] P. V. Hobbs, *Ice Physics*. Oxford, U.K.: Clarendon, 1974.
[34] W. J. Ellison, K. Lamkaouchi, and J. M. Moreau, "Water: A dielectric reference," *J. Mol. Liq.*, vol. 68, pp. 171–279, 1996.

Itai Hayut received the B.Sc. and M.Sc. degrees in physics and neuroscience from Ben-Gurion University of the Negev, Israel, in 2006 and 2008, respectively, and has been working toward the Ph.D. degree in Department of Applied Physics at the Hebrew University, Israel, since 2009.

His current work is focused on remote sensing from the human skin at sub-THz frequencies.

Alexander Puzenko was born in Russia, U.S.S.R., in 1944. He received the M.Sc. degree in radio physics and electronics and the Ph.D. degree in radio physics and quantum radio physics from the Kharkov State University (USSR) in 1966 and 1979, respectively.

From 1966 to 1983, he was with the Department of Radio Waves Propagation and Ionosphere of the Institute of Radiophysics and Electronics Ukrainian Academy of Sciences (Kharkov). From 1984 to 1994 he was with the Department of Space Radiophysics of Institute of Radio Astronomy National Academy of Science (Kharkov), as a senior scientist. In 1995 he immigrated to Israel, and since 1997, he has been with The Hebrew University of Jerusalem, where he is currently a senior scientist at the Dielectric Spectroscopy Laboratory in the Department of Applied Physics. His current research interests include time and frequency domain broad band dielectric spectroscopy, theory of dielectric polarization, relaxation phenomena, and strange kinetics in disordered materials, transport properties and percolation in complex systems, dielectric properties of biological systems and electromagnetic properties of human skin in the sub-THz frequency range.

Paul Ben Ishai received the Ph.D. degree from the Hebrew University in 2009.

For the last 12 years he has been involved with the Laboratory of Prof. Feldman, concentrating on dielectric research. He currently holds the position of Director of the Hebrew University's Center for Electromagnetic Research and Characterization, situated in the Applied Physics Department. His research topics include soft condensed matter physics, glassy dynamics, biophysics, sub-terahertz spectroscopy and dielectric spectroscopy. In 2004, he was part of the founding team investigating the interaction of the human sweat duct with sub terahertz electromagnetic radiation.

Alexander Polsman received the B.Sc. degree in physics from Racah Institute of Physics, The Hebrew University of Jerusalem, in 2009, and is currently working toward the M.Sc. degree at the Department of Applied Physics, School of Computer Science and Engineering, The Hebrew University of Jerusalem, Israel.

His research interests include microwave, millimeter- and submillimeter-wave technologies.

Aharon J. Agranat received the B.Sc degree in physics and mathematics, the M.Sc. degree in applied physics, and the Ph.D. degree in physics from the Hebrew University, Israel, in 1977, 1980, and 1986, respectively.

He is the N. Jaller Professor of Applied Science, the Director of the Brojde Center for Innovative Engineering and Computer Science, and the former Chairman of Applied Physics at the Hebrew University of Jerusalem. From 1986 to 1997, he was a senior research fellow at the California Institute of Technology, Pasadena. He is the author of over a hundred scientific papers, and holds over 25 patents.

Prof. Agranat is a Fellow of the Optical Society of America, and a recipient of the 2001 Discover Innovation Award in the area of communication for the invention of Electroholography.

Yuri Feldman was born in Kazan, U.S.S.R., in 1951. He received the M.S. degree in radio physics and the Ph.D. degree in molecular physics from the Kazan State University, U.S.S.R., in 1973 and 1981, respectively.

From 1973 to 1991, he was with Laboratory of Molecular Biophysics of Kazan Institute of Biology of the Academy of Science of the U.S.S.R. In 1991, he immigrated to Israel and since 1991, he has been with the Hebrew University of Jerusalem, where he is currently the Full Professor and the Head of the Dielectric Spectroscopy Laboratory. He also is a Director of the Center for Electromagnetic Research and Characterization (CERC) and since 2002 he is the Secretary and Member of the International Dielectric Society Board. He has spent over 30 years in the field and has more than 200 scientific publications related to dielectric spectroscopy and its applications. He holds 8 patents in the areas of electromagnetic properties of the matter. His current interests include broadband dielectric spectroscopy in frequency and time domain; theory of dielectric polarization and relaxation; relaxation phenomena and strange kinetics in disordered materials; electromagnetic properties of biological systems *in vitro* and *in vivo*.